Electronic Supplementary Material (ESI) for New Journal of Chemistry.


# An activation-free route to porous magnetic carbon adsorbents for the removal of phenolic compounds

Supplementary Data

Przemysław Strachowski[a], Wojciech Kiciński[b], Maciej Fronczak[a], Waldemar Kaszuwara[c], Piotr Baranowski[a], Michał Bystrzejewski,*[a]

[a]*Faculty of Chemistry, University of Warsaw, Pasteur 1 str., 02-093 Warsaw, Poland*
[b]*Military University of Technology, Urbanowicza 2 str., 00-908 Warsaw, Poland*
[c]*Faculty of Materials Science, Warsaw University of Technology, 00-141 Warsaw, Poland*
**Corresponding Author E-mail: mibys@chem.uw.edu.pl (Michał Bystrzejewski)*

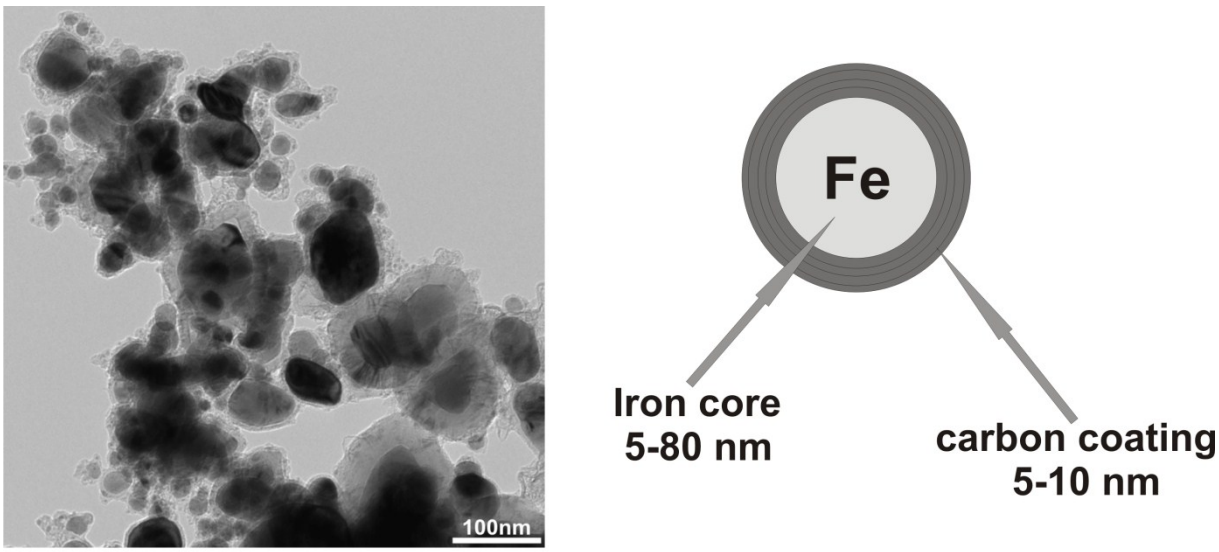


Figure S1. TEM image and scheme of structure of carbon encapsulated iron nanoparticles.

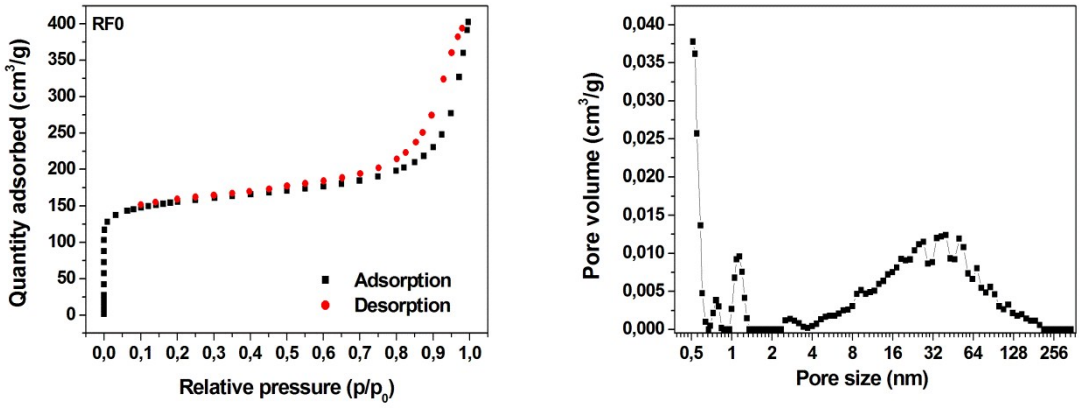


Figure S2. Low-temperature $N_2$ adsorption/desorption isotherm and pore size distribution of magnetic carbon xerogel RF0.

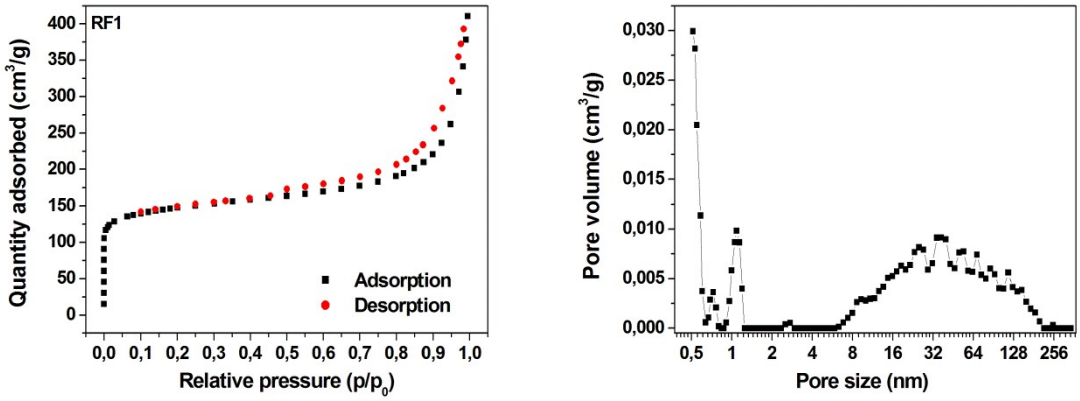


Figure S3. Low-temperature $N_2$ adsorption/desorption isotherm and pore size distribution of magnetic carbon xerogel RF1.

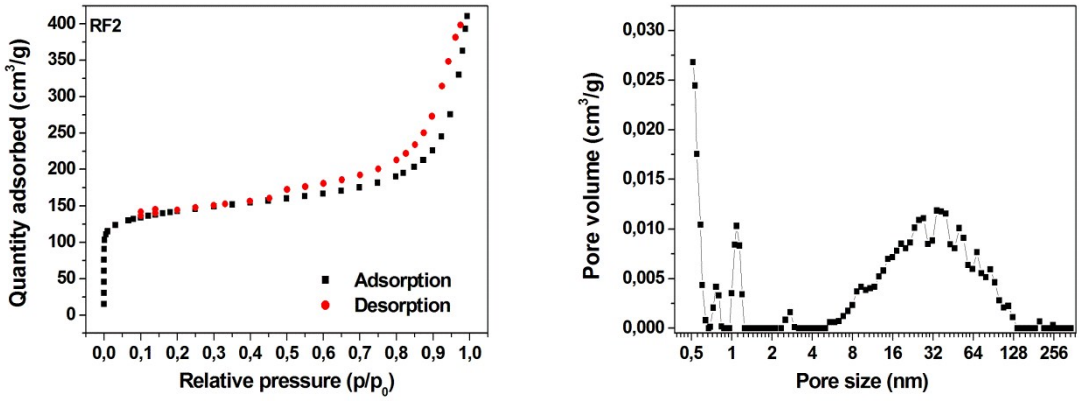


Figure S4. Low-temperature $N_2$ adsorption/desorption isotherm and pore size distribution of magnetic carbon xerogel RF2.

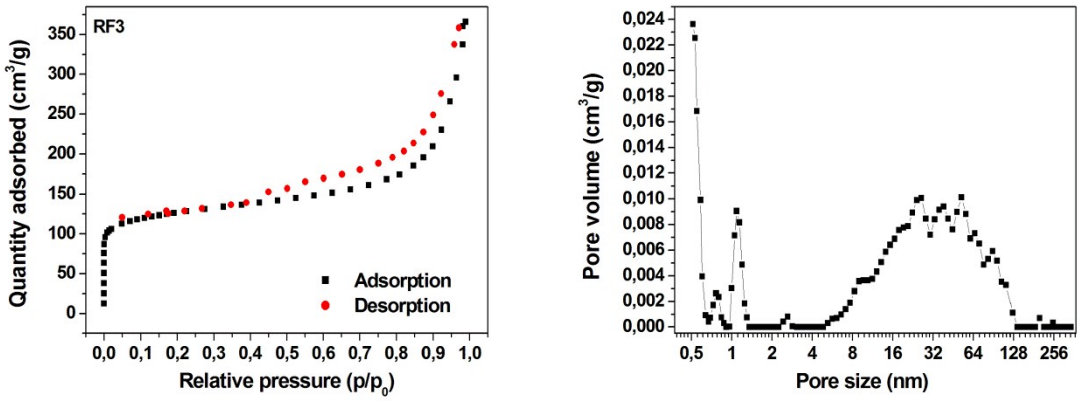


Figure S5. Low-temperature $N_2$ adsorption/desorption isotherm and pore size distribution of magnetic carbon xerogel RF3.

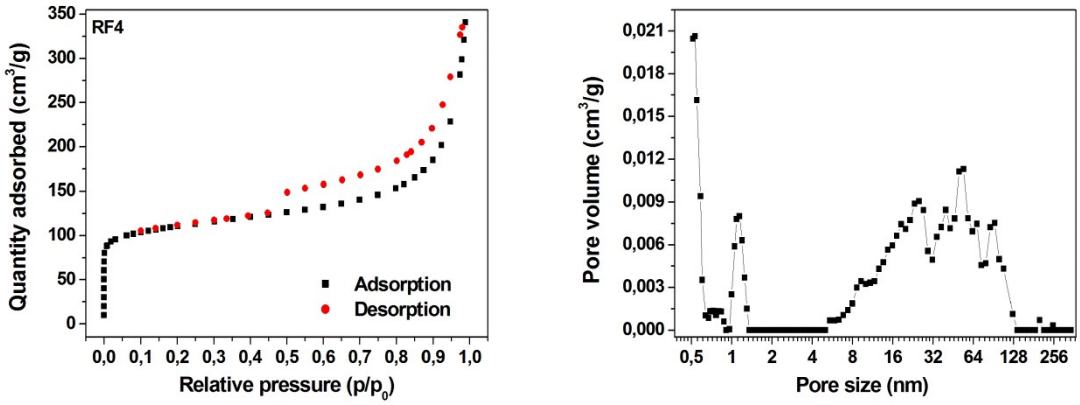


Figure S6. Low-temperature $N_2$ adsorption/desorption isotherm and pore size distribution of magnetic carbon xerogel RF4.

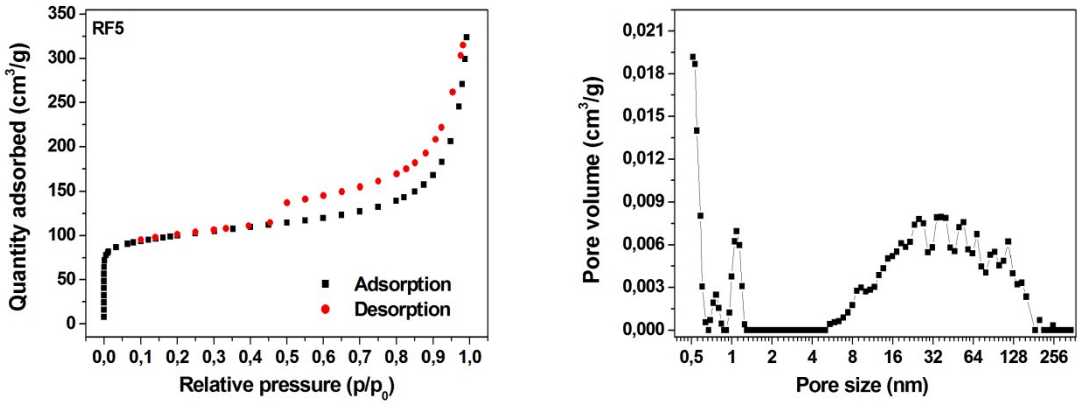


Figure S7. Low-temperature $N_2$ adsorption/desorption isotherm and pore size distribution of magnetic carbon xerogel RF5.

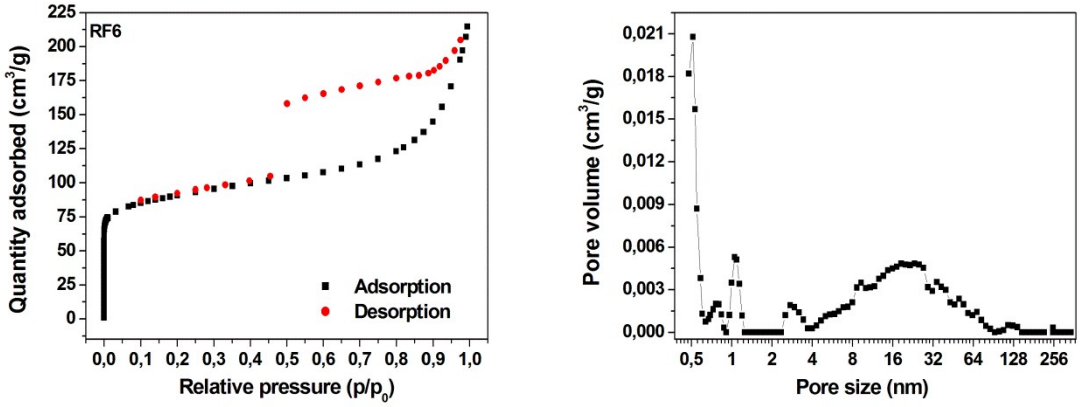


Figure S8. Low-temperature $N_2$ adsorption/desorption isotherm and pore size distribution of magnetic carbon xerogel RF6.

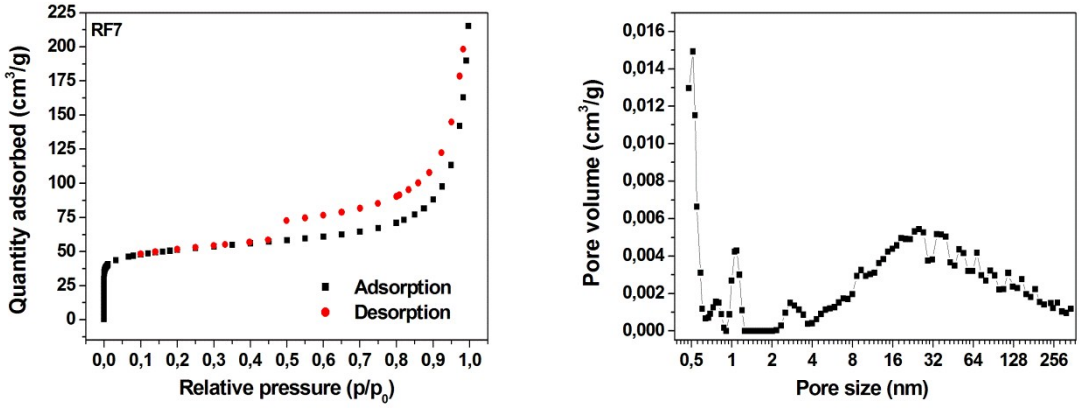


Figure S9. Low-temperature $N_2$ adsorption/desorption isotherm and pore size distribution of magnetic carbon xerogel RF7.

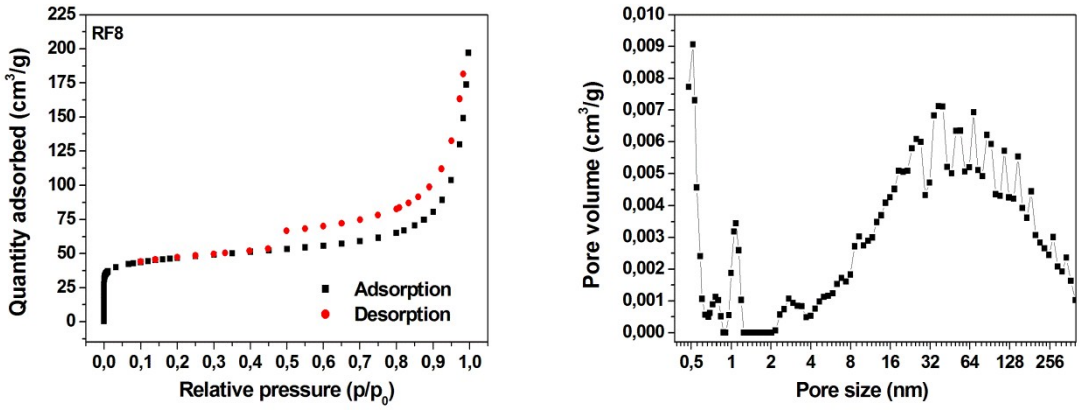


Figure S10. Low-temperature $N_2$ adsorption/desorption isotherm and pore size distribution of magnetic carbon xerogel RF8.

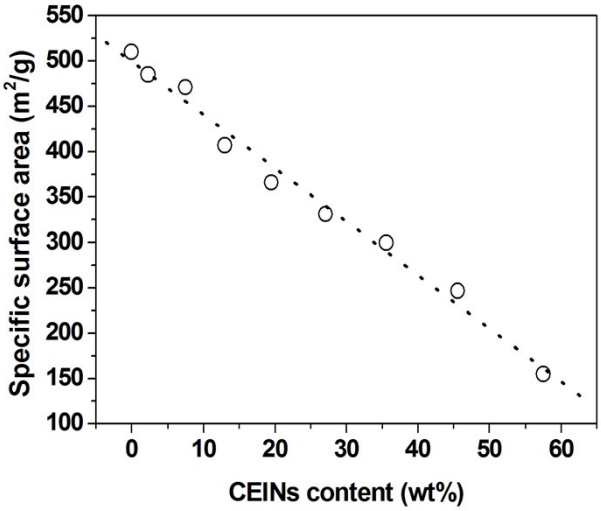


Figure S11. Specific surface area vs Fe content.

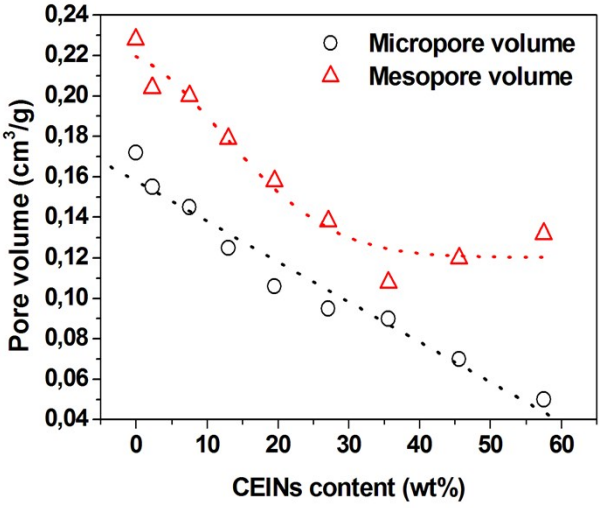


Figure S12. Micropore and mesopore volume vs CEINs content.

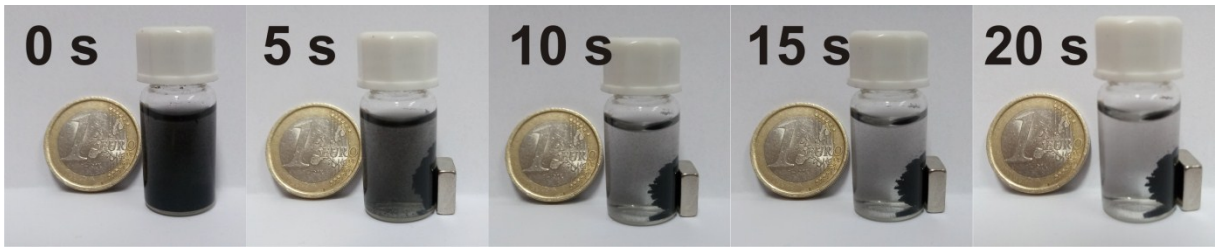


Figure S13. Separation of RF6 material from aqueous solution using a permanent magnet.

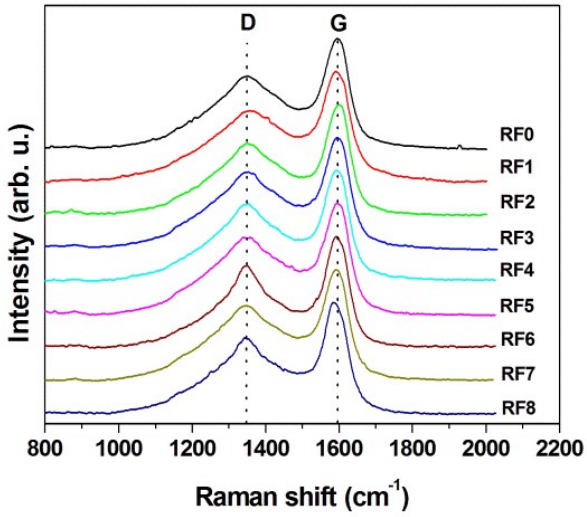


Figure S14. Raman spectra of magnetic carbon xerogels.

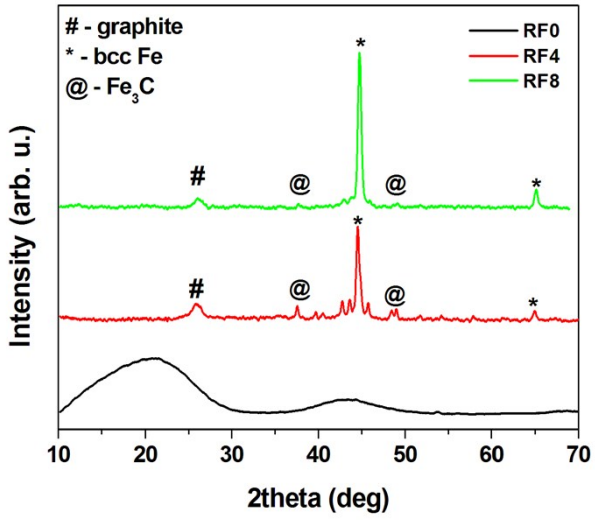


Figure S15. Powder XRD diffractograms of magnetic carbon xerogels.

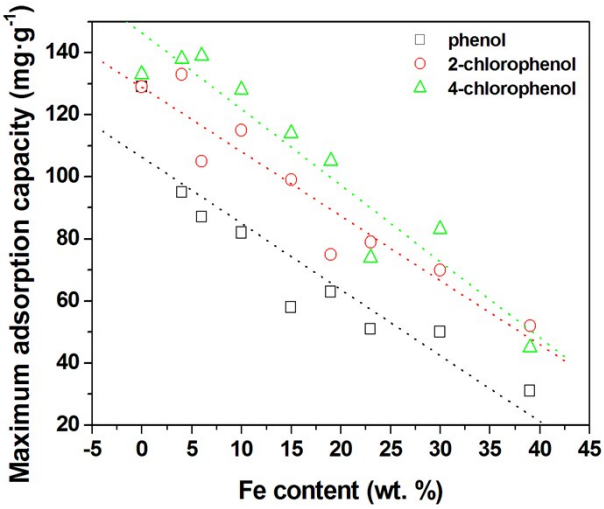


Figure S16. Maximum adsorption capacity vs Fe content in composite.

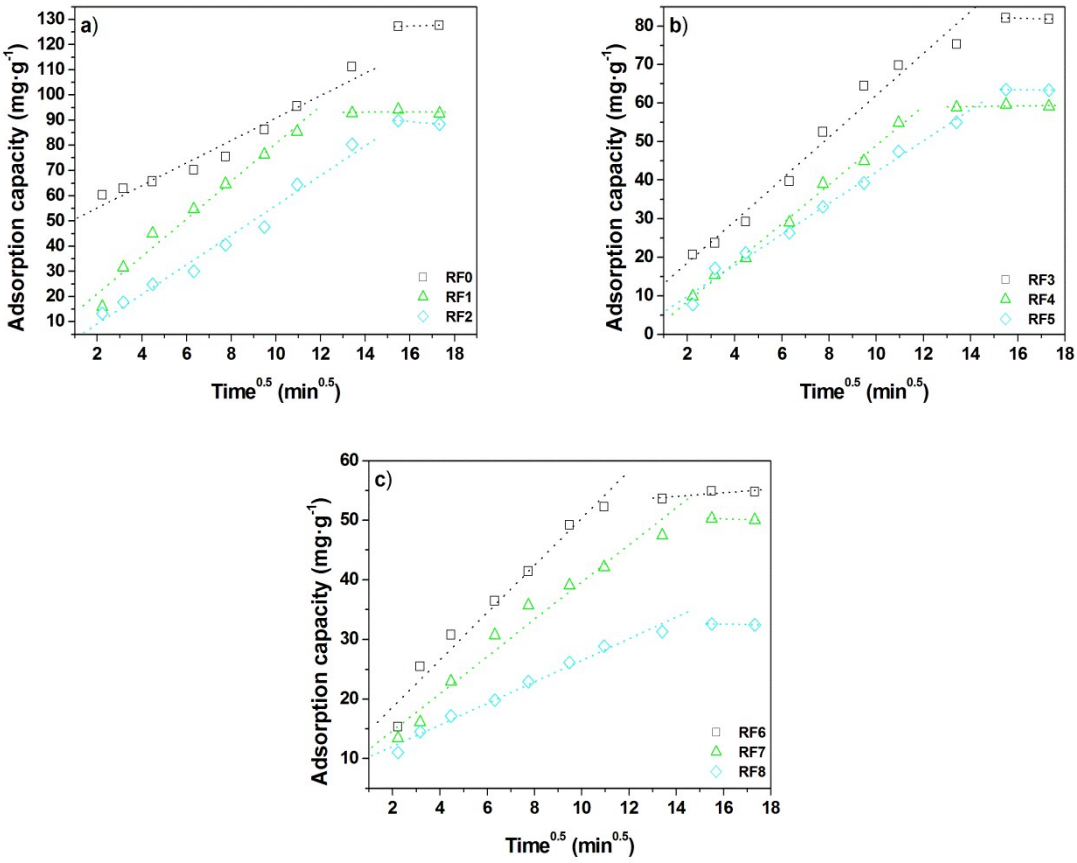


Figure S17. Intra-particle plots of adsorption kinetics of phenol

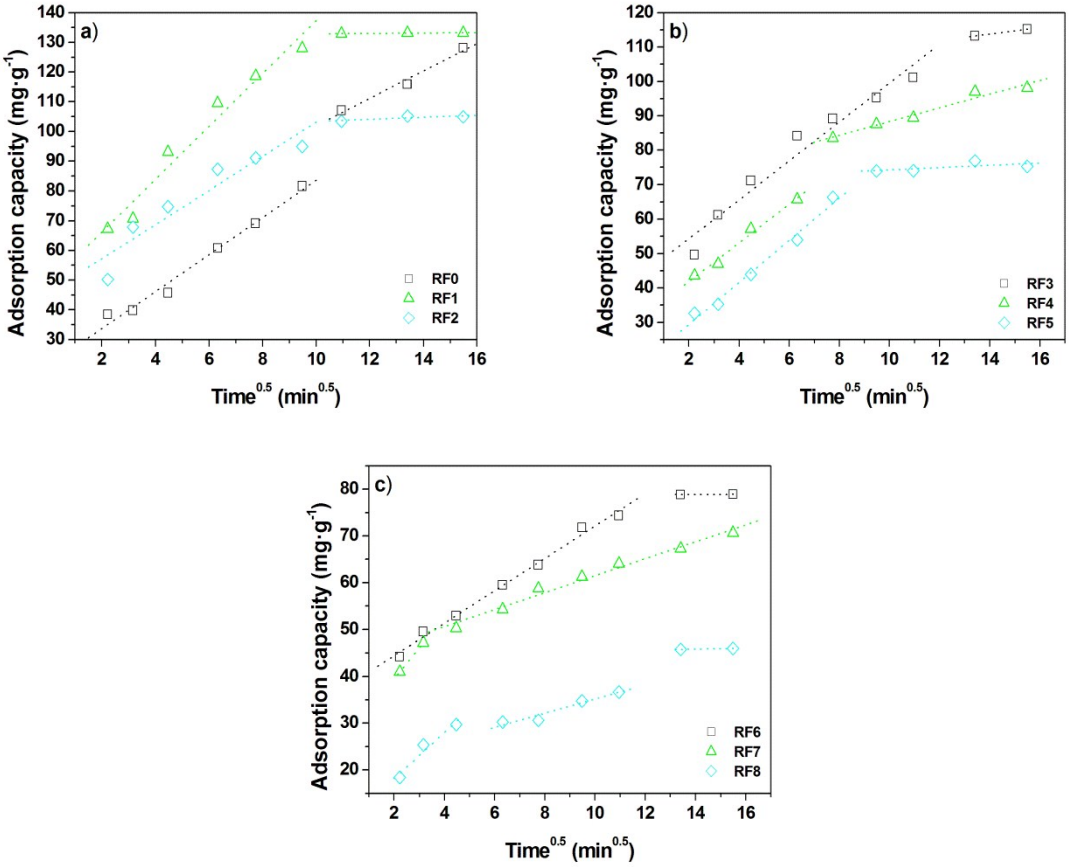


Figure S18. Intra-particle plots of adsorption kinetics of 2-chlorophenol

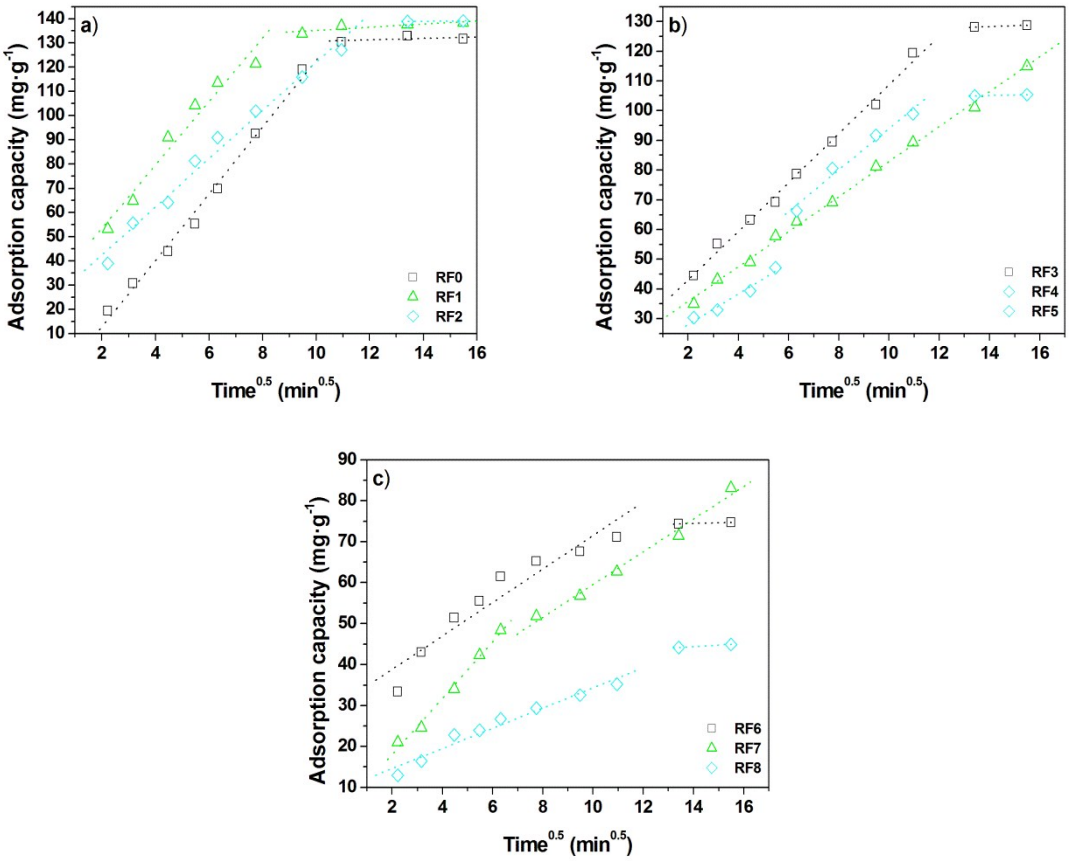


Figure S19. Intra-particle plots of adsorption kinetics of 4-chlorophenol